Heterogeneous & Homogeneous & Bio- & Nano-

CHEMCATCHEM

CATALYSIS

Accepted Article

Title: Effect of gold particles size onAu/C catalyst selectivity in HMF oxidation reaction

Authors: Cristina Megías-Sayago, Alice Lolli, Danilo Bonincontro, Anna Penkova, Stefania Albonetti, Fabrizio Cavani, Jose Antonio Odriozola, and Svetlana Ivanova

To be cited as: *ChemCatChem* 10.1002/cctc.201901742

Link to VoR: http://dx.doi.org/10.1002/cctc.201901742

A Journal of

ChemPubSoc Europe

WILEY-VCH

www.chemcatchem.org

Effect of gold particles size over Au/C catalyst selectivity in HMF oxidation reaction

C. Megías-Sayago[a], A. Lolli[b], D. Bonincontro[b], A. Penkova[a], S. Albonetti[b], F. Cavani[b], J. A. Odriozola[a] and S. Ivanova*[a]

Abstract: A series of gold nanoparticles in the 4-40 nm range were prepared, immobilized on activated carbon and further tested, at low base concentration, in the catalytic oxidation of 5-hydroxymethyl furfural (HMF) to 2,5- furandicarboxylic acid (FDCA). Gold particles size variation has no influence on HMF conversion but significantly affects product selectivity and carbon balance. This behavior is ascribed to the thermodynamically favorable oxygen reduction reaction on Au(100) faces. As the gold particle size decreases the Au(100)/Au(111) exposure ratio, estimated by using the van Hardeveld - Hartog model, increases as well as the FDCA selectivity. The smaller the gold particle size the smaller the 5-hydroxymethyl-2-furancarboxylic acid (HMFCA) to FDCA ratio pointing to the gold size dependent behaviour of the oxidation of the alcohol function of the HMF molecule.

Introduction

Progressive substitution of petroleum-based chemicals by sustainable bio-based products should be the result of renewable lignocellulosic biomass valorization through molecules able to replace those employed nowadays. Lignocellulosic components are rich sources of platform chemicals available for dehydration, hydrogenation and/or oxidation reactions in separate or in consecutive manner. 2,5- furandicarboxylic acid (FDCA) is a very good example of such chemical. FDCA is a potential substitute of terephtalic acid, used for polyethylene terephthalate plastics production, because of their structural similarity and final plastics properties alikeness [1,2]. Its synthesis route follows a set of consecutive ractions including biomass depolimerization, hexoses isomerization and dehydration to 5-hydroxymethyl furfural (5-HMF) and oxidation to the final FDCA product.

5-HMF to FDCA selective oxidation occurs either in homogeneous conditions, using $KMnO_4$ or metal halides [3–5] or over noble metals based heterogeneous catalysts [6–8]. Within the group of catalytically active noble metals in oxidation reactions, particular interest awakes gold, longtime considered as a metal with poor ability to activate oxygen. However, more and more studies demonstrates that gold – oxygen interactions are controlled by the support nature or by the size of the metal clusters [9–11], in such a way that the higher the gold dispersion the higher the overall oxidation reaction rate. For gas phase oxidation reactions dioxygen activation by the catalyst, either bare gold or supported on non-reducible oxides or carbon, involves charge transfer from Au to O_2. This results in an increase of the O-O bond distance appearing superoxo-like species (O_2^-) probably accompanied by partially reduced gold that is very difficult to detect as purely cationic states since important electronic structure rearrangements [12,13].

Liquid phase oxidation reactions on gold behave quite differently. In liquid media, dioxygen-solvent interactions must be considered. Fristrup et al. [14] studied the gold-catalyzed aerobic oxidation of aldehydes in methanol. These authors reported that dioxygen was not directly involved in the oxidation process but indirectly after reacting with the solvent. Similar results were found in an aqueous solution, dioxygen reacts indirectly as hydroxide ions generated upon O_2 dissolution [15]. Aldehyde and alcohol function oxidations occur by H-abstraction in the functional group to be oxidized mediated by the O_2-generated hydroxide species.

The HMF oxidation path to FDCA may be schematized considering three different steps (scheme 1): i) the fast oxidation of the aldehyde to carboxylic group resulting in 5-hydroxymethyl-2-furancarboxylic acid (HMFCA) and ii) a two-step oxidation of the HMFCA species including the slow oxidation of the alcoholic function to aldehyde given rise to, 5-formyl-2-furancarboxylic acid (FFCA) and, in a further fast reaction step, the oxidation of the dialdehyde to 2,5-furan dicarboxylic acid (FDCA). As long as the OH^- are present or generated in the media the HMF oxidation occurs selectively towards the final product.

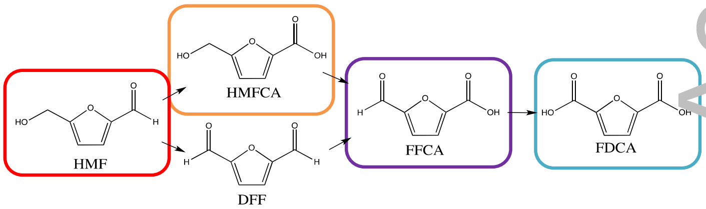

Scheme 1. Reaction path for HMF oxidation to FDCA.

In this study HMF is used as model molecule to study the size dependent ability of gold catalysts on the oxidation of alcohol (aldehyde) functions. This will provide clues on the dioxygen activation mechanism on gold and clarify its participation in the

---

[a] Dr. C. Megías-Sayago, Dr. A. Penkova, Prof. J. A. Odriozola and Dr. S. Ivanova
Department: Departamento de Química Inorgánica e Instituto de Ciencia de Materiales de Sevilla
Institution: Universidad de Sevilla-CSIC
Address: Américo Vespucio 49, 41092, Seville, Spain
E-mail: svetlana@icmse.csic.es
[b] Dr. A. Lolli, D. Bonincontro, Prof. S. Albonetti, Prof. F. Cavani
Department Dip. di Chimica Industriale “Toso Montanari”,
Institution: Università di Bologna
Address: Viale del Risorgimento, 4, 40136 Bologna BO, Italy

Supporting information for this article is given via a link at the end of the document.((Please delete this text if not appropriate))

10.1002/cctc.201901742

reaction. For ensuring that the results are not altered by support properties or gold loading the same support and similar Au loadings are used.

Results and Discussion

The gold nanoparticles synthesis parameters are chosen in such a way that a wide range of particle sizes may be obtained. A selection of gold early prepared and already reported by us are used in this study [16]. A typical example of the preparation method is presented in the experimental section and the resulting gold colloids preparation conditions, gold loadings and average particle sizes summarized in table 1.

Table 1. Selected samples, preparation, parameters, corresponding gold loadings, and particle sizes.

Sample	PVA[a]:Au:NaBH$_4$[b] ratio	Au loading, wt.%	Particle size, nm[a]
AuC_I	0.85:1:5	2.3	4.8
AuC_II	0.85:1:10	2.3	6.6
AuC_III	0.5:1:5	2.4	8.7
AuC_IV	0:1:5	2.0	15.4
AuC_V	0.85:1:10	2.1	37.9

[a] PVA:Au weight ratio, [b] Au:NaBH$_4$ molar ratio; [c] measured by TEM

Figure 1 summarizes the HMF conversion and product selectivity as a function of the gold particle size.

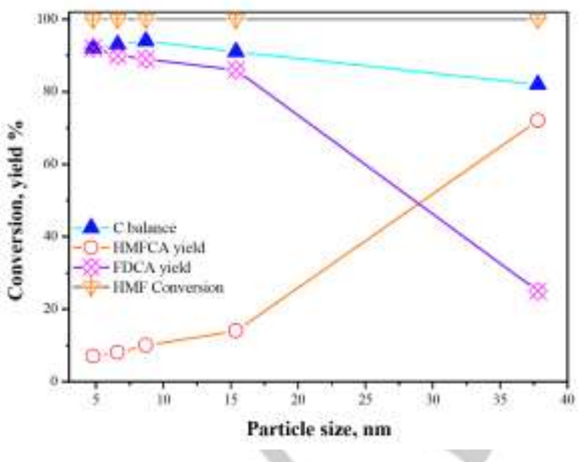

Figure 1. Gold catalysts screening: HMF conversion and HMFCA, FDCA yields vs. mean particle size. Reaction conditions: HMF:Au:NaOH molar ratio 1:0.01:2, 10 bar O_2, 70 ºC, 400 rpm, 4h.

Conversion of HMF to FDCA on gold catalysts proceeds through preferential aldehyde group oxidation to HMFCA and subsequent alcohol group oxidation to FFCA finally transformed into FDCA. Aldehyde group oxidation is a rapid process and normally the FFCA intermediate is absent at the final reaction time. Within the series, no matter the gold particle size, all catalysts lead to full HMF conversion and only HMFCA and FDCA are detected as products. On the other hand, the product selectivity and C balance are significantly affected by the particle size. It is interesting to underline that in the 4-16 nm particle size only minor changes in selectivity are observed disfavoring FDCA for HMFCA. However, for particle sizes higher than 35 nm HMFCA is the primary product. It seems that aldehyde group oxidation to HMFCA is less size dependent than alcohol group oxidation. The oxidation rate of alcohol function slightly decreases with particle size in the 4-16 nm range and dramatically for the highest particle size tested. A question raises, what is making the difference? Full HMF conversion is always attained; therefore, its concentration is not a factor in these conditions. Let's consider the presence of base and oxygen.

It is well known that, in basic conditions (1:2 HMF:OH$^-$ molar ratio in our experiments), aldehyde groups transform to alkoxide intermediates trough nucleophilic addition of hydroxide ion and subsequent proton transfer from water [17,18]. When catalyzed this reaction goes selectively to carboxylic acid but in absence of catalysts Cannizaro reaction occurs and the aldehyde (HMFCA) transforms in the corresponding alcohol and carboxylic acid. Oxidation of alcohols are reported to occur by H-abstraction from the OH group by hydroxide ions [15,19]. The base concentration used in these experiments, two base equivalents, is not enough to complete the reaction unless its concentration were continuously renewed. On reducing the OH$^-$ concentration (Figure 2) the HMFCA is the main product although FDCA is also found. The presence of both suggests that base is helping in all processes and that the reaction rate of aldehyde oxidation over gold is higher than that of alcohols, this is also confirmed by the absence of 2,5-Diformylfuran (DFF). It is worth underlining that HMF conversion and HMFCA production are almost equimolar suggesting that the first process is using the starting excess of base before all the other processes and that a full conversion of HMF will be always observed when an initial OH$^-$ concentration equal or superior to that of HMF is employed. It should be noted that HMF is not converted in absence of base.

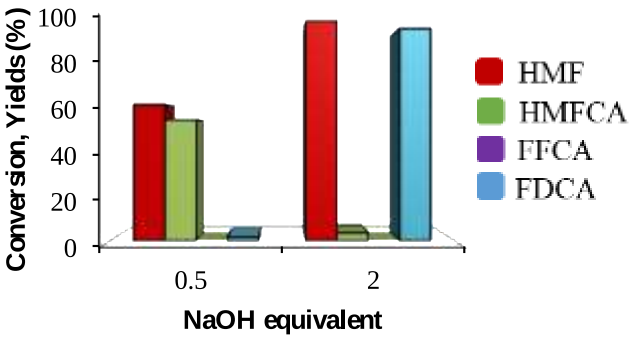

Figure 2. Conversion/yield dependence on base equivalent over AuC_II sample. Reaction conditions: HMF:Au:NaOH molar ratio 1:0.01:0.5 or 1:0.01:2, respectively, 10 bar O_2, 70 ºC, 400 rpm, 4h.

10.1002/cctc.201901742

At this point, a new charge of OH^- is necessary for all other steps. Here is where oxygen enters in the equations. Davis et al. [20] found using labled oxygen that it is involved in the oxidation of alcohols although not directly incorporated from dioxygen but from OH^- groups present in the reaction media. They conclude that the role of dioxygen is indirect as regenerator of the hydroxide ions. The only way to generate hydroxides from O_2 in aqueous media is its reduction. Two possible ways of oxygen reduction in alkaline media are reported, 2-electron reduction with the formation of peroxide ions

$$O_2+H_2O+2e^- \rightarrow HOO^-+OH^-$$

and 4-electron reduction

$$O_2 +2H_2O+4e^- \rightarrow 4OH^-$$

The latter just observed on Au (100) surfaces and its vicinals. This reaction is of particular interest since Au (100) surfaces are the most active known catalyst for the 4-electron O_2 reduction [21–24] and relative exposure of the (100) face of FCC nanoparticles is size dependent. The application of electrochemical potential is generally required for running this reaction, although on small gold nanoparticles, *i.e.* with high Au (100) surface exposure and high OH^- coverage, the oxygen reduction reaction is thermodynamically favorable. In addition, the oxidation of aldehydes (2-electron oxidation) and that of alcohols (4-electron oxidation) to carboxylic acid assures the necessary electrons.

Considering that gold is an fcc metal and expose (111) and (100) surfaces (Figure 3 inset), every change in its size will produce a change in its (100)/(111) surface ratio. Using the model of van Hardeveld and Hartog [25] the surface atoms and sites corresponding to both surfaces and their relation with the experimental average particle size can be estimated (Figure 3).

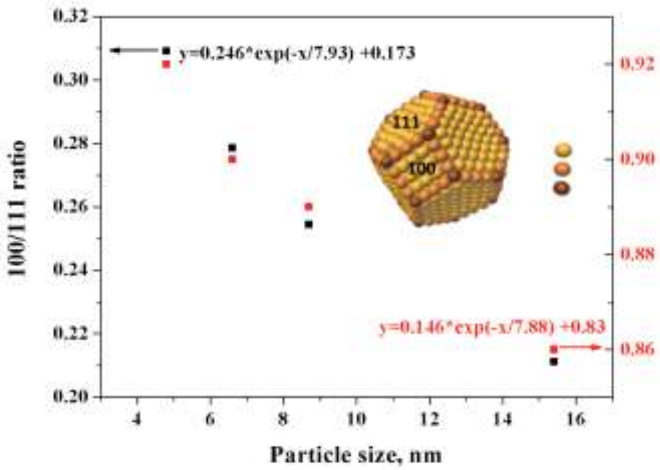

Figure 3 100/111 surface ratio for the studied samples and FDCA selectivity dependence on particle size.

The 100/111 gold surface ratio decreases exponentially with particles size as FDCA selectivity does. A 1st order exponential decay expression fits both tendencies with the same value for the exponent suggesting a direct relationship between the processes involved over Au (100) surface and FDCA production. If we consider that at high 100/111 ratio the 4-electron oxygen reduction occurs with hydroxide ions as a product, the oxidation of HMFCA proceeds and the FDCA yield is higher. All processes need base, O_2 reduction and alcohol/aldehyde oxidation. The Au (100) surfaces must be covered by OH^- to produce $AuOH_{ads}$ in order to reduce the potential of O_2 to HOO^- and to OH^- 2nd step reduction [26]. So, for hydroxide ion generation (O_2 activation) over gold we need preferential exposure of the Au (100) face, *i.e.* particles as small as possible and presence of base in order to promote the 4-electrons O_2 reduction and to renew continuously the hydroxide ions concentration required to accomplish the reaction to FDCA. The latter means that for very high base excess the oxidation reaction may proceed using the hydroxide ions from the media and probability should not be size dependent. However in the absence of base, when the oxygen reduction reaction is not thermodynamically favorable, the FDCA production proceeds via direct oxidation of HMFCA. The rate of this reaction increases linearly with the surface gold concentration needed to dehydrogenate HMFCA and further convert it in FDCA [27].Both facts, suggest that FDCA production is size dependent at low to moderate base concentration and independent in the limiting cases, absence or great excess of base.

Two samples were selected, AuC_II and AuC_III to analyze the stability of the catalysts. Both samples are submitted to 4 reaction cycles keeping the HMF:Au:NaOH ratio constant (Figure 4). Our previous study on the deactivation behavior of these systems [28] in the glucose to gluconic acid oxidation reveals that a particle size increase occurs after the reaction 1st cycle remaining then constant till the 4th cycle. The same behavior is observed in this study during the cycles of HMF oxidation. The gold particle size of the AuC_II catalyst increases from 6.6 to 8.8 nm and that of AuC_III one from 8.7 to 12.2 nm. Figure 5 shows TEM images and particle size distributions for both catalysts after the 4th cycle.

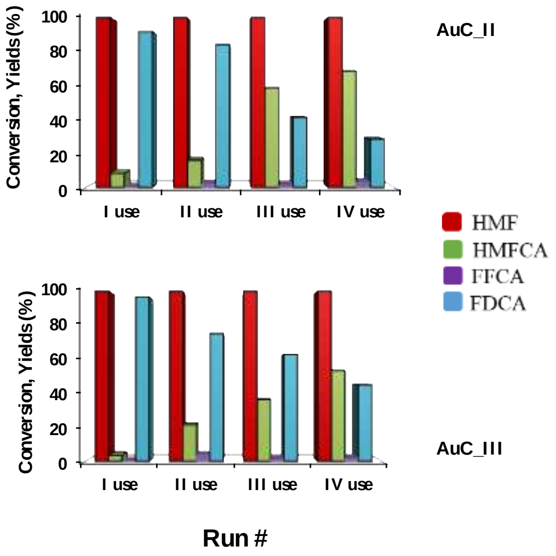

Figure 4. Reuse of AuC_II and AuC_III sample. Reaction conditions: HMF:Au:NaOH molar ratio 1:0.01:0.5 or 1:0.01:2, respectively, 10 bar O_2, 70 ºC, 400 rpm, 4h.

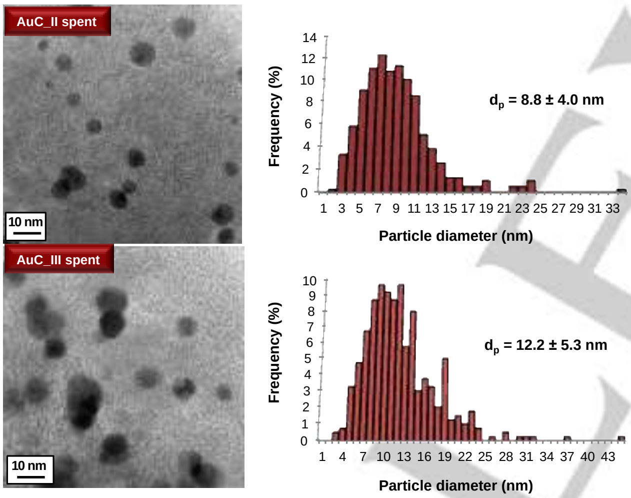

Figure 5. Representative TEM images and gold particle size distributions of AuC_II and AuC_III spent samples after 4 cycles.

If our theory for size dependent O_2 reduction and related FDCA formation is true all reaction cycles after the 1st one; should give similar FDCA selectivity to those measured for samples with similar particle sizes whatever the initial size and reaction cycle. The spent AuC_II catalyst (8.8 nm) and the fresh AuC_III one (8.7 nm) present the same selectivity to FDCA, 90 and 89%, respectively. For catalysts AuC_III (spent, 12.2 nm) and AuC_IV (fresh, 15.4 nm) the selectivities to FDCA are also similar, 86 and 75 % respectively. However, in the 3rd and 4th cycle the catalysts continue losing selectivity to FDCA. This change in the oxidation selectivity is independent of the gold particle size and could be ascribed to a continuous change in the symmetry of the Au (100) surface from four-fold to six-fold layers [28]. This change causes a decrease in the OH^- adsorption on Au (100) inhibiting the 4-electron reduction, *i.e.* Au (100) surface starts to behave as Au (111) surface. Hausen et al. [29] reported a higher reconstruction rate for Au (100) surfaces than for Au (111) ones. This reorganization, described as network of dislocations, produces important changes on surface' electric potential altering its electronic properties and negatively affect OH^- adsorption behavior and reactivity. The concentration of $AuOH_{ads}$ species decreases as O_2 reduction reaction rate and FDCA selectivity does. It appears that subtle change in particle size greatly affects gold behavior for O_2 activation being much more noticeable for the smallest gold particle size catalysts. Au 4f level XPS spectra of AuC_I and AuC_V catalysts, as representatives for the lowest and highest particle size samples, are plotted in Figure 6. The binding energy of $4f_{5/2}$ and $4f_{7/2}$ levels peak at 88.2 and 84.5 eV, respectively, indicating the presence of metallic gold. Changes inn the bining energy for the spent catalysts are hardly noticeable, but the sintering behavior of the gold particles upon reaction is clearly seen by the intensity decrease observed for the spent AuC_I catalyst. Figure 7 plots XPS difference spectra. The high-resolution O 1s XPS spectrum of fresh samples is subtracted from the one of the spent catalyst. An increase of the number of surface oxygen species is observed after reaction for both AuC_I and AuC_V catalysts. The concentration of O-containing species on the catalyst surface is lower for the catalyst with smaller gold particle size. The differences result in broad signals suggesting a wide variety of adosrbed species. The XPS difference spectrum of gold catalyst with the biggest particle size, AuC_V, presents a main contribution at ~ 531 eV with a second maxima of lower intensity at ~534 eV. The difference spectrum of the catalyst with the smallest particle size, AuC_I, presents just one maximum peaking at ~532 eV, although its complex shape suggests the existence of more than one species. All the signals in this energy range may be ascribed to the presence of C-O, C=O and/or C-OH bonds in the adsorbed species [31, 32], i.e. sodium carboxylates or esters present bonds that typically appears in this region suggesting the presence of intermediates and/or products on the catalyst surface after reaction [33,34]. The latter should be expected since for AuC_V, the biggest gold particle size catalyst, the C-balance is the lowest observed. This suggests that the adsorption/desorption behavior on the catalyst surface is also affected by gold particle size. Higher the gold particle size lower the reaction rate and higher the products/intermediates adsorption.

10.1002/cctc.201901742

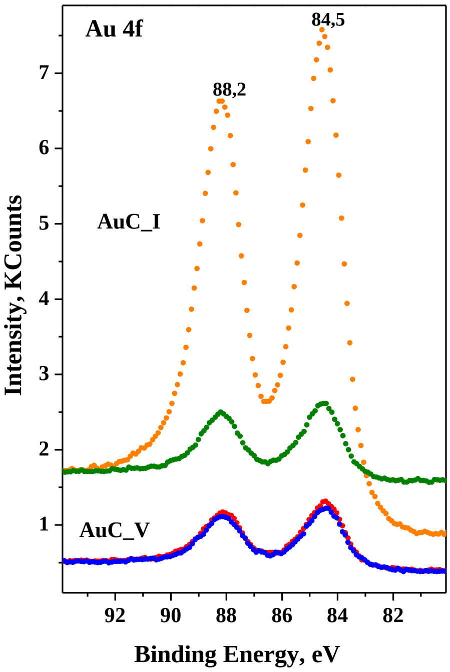

Figure 6. XPS spectra of Au 4f of fresh and spent.

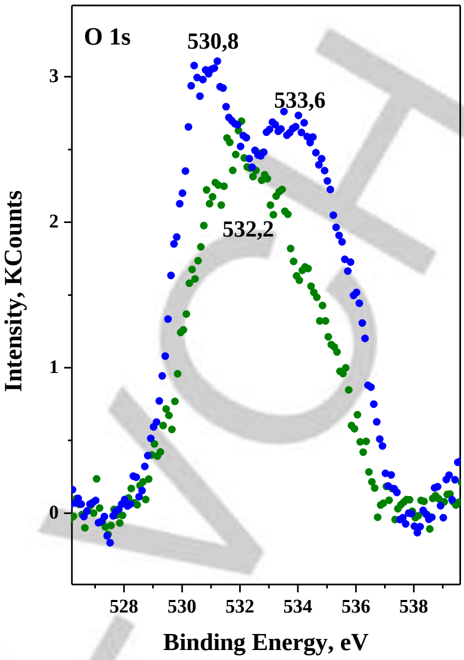

Figure 7. XPS spectra difference of O 1s (spent – fresh sample) for AuC_I and AuC_V catalysts.

The activity of gold in low base environments is conditioned by the presence of hydroxide ions, either added as base or produced via 2e$^-$ or 4e$^-$ O_2 reduction. This reaction is thermodynamically favorable over small size gold nanoparticles having the highest percentage of Au (100) surface faces exposed. That surface accelerates the 4-electron oxygen reduction reaction, increases significantly the hydroxide ion concentration, and influences positively the alcohol/aldehyde oxidation rate. It is important to underline that this model applies only for particles within the 4-20 nm range. Bigger particles do not fulfill this relationship and other mechanisms should be applied. The latter is also confirmed by the important change of the C balance for the sample AuC_V. This C-loss is either produced by covering gold surface with intermediates or by Cannizaro reaction products (although not detected during the analysis).

Conclusions

By studying as a function of gold particle size the catalytic oxidation of HMF to FDCA at low base concentration using O_2 as oxidant, the structure sensitivity of this reaction is analyzed. Whatever the gold particle size, full conversion of HMF is attained. However, product selectivity and carbon balance depend on gold particle size. The catalytic behavior of gold nanoparticles in the 4-40 nm size range may be split in two groups, selectivity to FDCA and carbon balances above 85% that slightly decrease on increasing the particle size are observed for the smaller gold particles (4-16 nm range). Above 16 nm gold particles the carbon balance and selectivity strongly decrease. The same tendency is observed for the dependence of the FDCA yield and the Au(100)/Au(111) exposure ratio on the gold particle size that fit an exponential decay trend on increasing particle size. The obtained results evidence that the oxidation of the alcohol function of the HMFCA intermediate depends on gold particle size sensitive and, therefore, structure-sensitive. The structure sensitivity of this reaction is directly related to the oxygen reduction ability and base concentration. The reaction yield to FDCA is higher for the smallest gold particle sizes since the 4-electron oxygen reduction is thermodynamically favorable.

Experimental Section

Catalyst series

The samples used in this study are selected from a series of previously reported catalysts [16]. In a typical preparation, 5.10^{-4} M $HAuCl_4$ (Johnson Matthey) aqueous solution is stirred together with a polyvinyl alcohol solution (PVA, 1 wt.% in water), used as stabilizer, for 20 min at 600 rpm (room temperature). Afterwards, an appropriate amount of 0.1 M freshly prepared $NaBH_4$ solution was added to reduce the gold precursor. The preformed colloid (2wt% Au nominal value) is immobilized on commercial activated charcoal Darco© (Sigma Aldrich, 100 mesh). After ageing for 45 min, the resulting solid was recovered by centrifugation, filtered, dried and finally calcined in static air at 300°C for 2 h. The gold particle size is modified by wisely selecting different Au:PVA:$NaBH_4$ ratios. This allows selecting a series of catalysts s with mean particle size in the 4-40 nm range. The selected catalysts, the Au:PVA:NaBH4 ratios used for their preparation, their mean particle size and actual gold loadings are summarized in table 1.

High specific surface area (968 m^2/g) activated charcoal is used in this study with dominant microporosity. The activated charcoal presents low to moderate acid character, which decrease with gold metal addition [35]. A blank test of the reaction over this charcoal does not produce any products but an adsorption of around 8 % of the initial HMF.

Characterization

Gold loadings were measured by using a Horiba Jobin Yvon ICP spectrometer.

Transmission electron microscopy (TEM/STEM) studies on particle size and dispersion of the catalysts were performed on a FEI TECNAI F20 microscope operating at 200keV. The average gold particle size was estimated based on surface distribution calculations as shown in equation 1:

$$D\,[3,2] = \frac{\sum_1^n \mathrm{D}_i^3 v_i}{\sum_1^n \mathrm{D}_i^2 v_i} \tag{1}$$

where D_i is the geometric diameter of the i^{th} particle, and v_i the number of particles with this diameter. The particle size distribution is evaluated using over 200 particles for every sample.

XPS measurements were carried out on SPECS spectrometer equipped with PHOIBOS 150 MCD analyzer working with fixed pass energy of 40 eV and 0.1 eV resolution for the studied zones. As monochromatic source of radiation Al Kα radiation (1486.6 eV) was used working on 250W and 12.5 kV voltage. The analytical chamber operates at ultra-high vacuum at around 10^{-10} mbar pressure. Prior use the samples were pressed into a thin disk. The XPS spectra were recorded at room temperature and the binding energy was calibrated on C1s at 284,6 eV with an uncertainty ±0.2 eV.

Catalytic tests

The oxidation of HMF was carried out in a 100 mL volume autoclave reactor, provided with mechanical stirrer and temperature/pressure controllers. In a typical experiment, the reactor was charged with an aqueous solution of HMF (approx. 25 mL, 0.08 M), the necessary amount of NaOH, and the catalyst in the HMF:Au:NaOH ratio of 1:0.01:2. Before test, the reactor was purged twice with pure O_2 (10 bar) and finally pressurized to 10 bars. The variation of the oxygen pressure (Figure SI. 1) shows that in the 7-15 bars pressure range no mass transfer limitations occur being 10 bars sufficient to assure oxygen availability without influencing the product distribution. After pressurizing, the temperature was raised to 70ºC and the reaction mixture was stirred at approximately 400 rpm for 4 hours. Then the reactor was introduced into an ice bath and the reaction mixture was centrifuged and filtered. Afterwards, a sample was taken and diluted before the test in an Agilent Infinity 1260 liquid chromatograph equipped with a DAD detector and an Aminex HPX-87H 300 mm × 7.8 mm column using 0.005 M H_2SO_4 as eluent. The stability was studied over the spent samples recovered from the post-reaction mixture and dried at 120ºC overnight. The samples were used directly after drying without any further treatment in a newly charged reactor with HMF:Au:NaOH molar ratios kept constant. Conversion, selectivity and yields are calculated after calibration using as reference commercial samples, according to the following equations:

$$\text{Conversion (\%)} = \frac{[\mathrm{HMF}]_\mathrm{F} - [\mathrm{HMF}]_\mathrm{I}}{[\mathrm{HMF}]_\mathrm{F}} \text{ x } 100 \tag{2}$$

$$\text{FDCA Selectivity (\%)} = \frac{\text{FDCA mols}}{\text{HMF mols}_\mathrm{I} - \text{HMF mols}_\mathrm{F}} \text{ x } 100 \tag{3}$$

$$\text{FDCA Yield (\%)} = \frac{\text{Conversion}}{100} \text{ x Selectivity} \tag{4}$$

Acknowledgements

Financial support has been obtained from the Spanish Ministerio de Ciencia, Innovación y Universidades (ENE2017-82451-C3-3-R) co-financed by E.U. FEDER funds.

Keywords: HMF oxidation, 2,5-furandicarboxylic acid, gold catalysts, size/selectivity dependence

References

[1] A. Gandini, A. J. D. Silvestre, C. P. Neto, A. F. Sousa, M. Gomes, J. Polymer Scie.: A: Polymer Chem., 2009, 47, 295–298;
[2] M. Gomes, A. Gandini, A. J. D. Silvestre, B. Reis, J. Polymer Scie.: A: Polymer Chem., 2011, 49, 3759–3768
[3] W. Partenheimer, V. V. Grushin, Adv. Synth. Catal. 2001, 343, 102–111.
[4] L. Ardemani, G. Cibin, A. J. Dent, M. A. Isaacs, G. Kyriakou, A.F. Lee, C. M. A. Parlett, S. A. Parryb , K. Wilson Chem. Sci, 2015, 6, 4940–4945.
[5] A.S. Amarasekara, D. Green, E. McMillan, Catal. Commun., 2008, 9, 286–288.
[6] S. E. Davis, L. R. Houk, E. C. Tamargo, A. K. Datye, R. J. Davis, Catal. Today, 2011, 160, 55-60.
[7] M. Ventura, A. Dibenedetto, M. Aresta, Inorg. Chim. Acta, 2018, 470, 11–21.
[8] S. Albonetti, A. Lolli, V. Morandi, A. Migliori, C. Lucarelli, F. Cavani, Appl. Catal. B: Environm., 2015, 163, 520-530.
[9] M. Boronat, A. Corma, Dalton Trans., 2010, 39, 8538–8546.
[10] N. López, J. K. Nørskov, J. Am. Chem. Soc., 2002, 124, 11262-11263.
[11] T. Jiang, D. J.Mowbray, S. Dobrin, H. Falsig, B. Hvolbæk, T. Bligaard, J. K. Nørskov, J. Phys. Chem. C, 2009, 113, 10548-10553.
[12] J.A. van Bokhoven, C. Louis, J. T. Miller, M. Tromp, O. V. Safonova, P. Glatzel, Angew. Chem. Int. Ed., 2006, 45, 4651 –4654.
[13] A.P. Woodham, G. Meijer, A. Fielicke, J. Am. Chem. Soc., 2013, 135, 1727-1730.
[14] P.Fristrup, L. Bahn Johansen, C.H. Christensen, Chem. Commun., 2008, 2750–2752

[15] B. N. Zope, D. D. Hibbitts, M. Neurock, R. J. Davis, Science, 2010, 330, 74.

[16] C. Megías-Sayago, J.L. Santos, F. Ammari, M. Chenouf, S. Ivanova, M.A. Centeno, J.A. Odriozola, Catal. Today, 2018, 306, 183-190.

[17] K.P.C. Vollhardt, N.E. Schore Organic Chemistry 2nd Ed., W.H. Freeman and Company

[18] S. Warren, Chemistry of the carbonyl group: a programmed approach to organic reaction mechanisms. Wiley, 1974.

[19] C. Shang, Z.-P- Liu, J. Am. Chem. Soc., 2011, 133, 9938-9947.

[20] S. E. Davis , B. N. Zope, R. J. Davis, Green Chem., 2012, 14, 143-147.

[21] R.R. Adzic, N.M. Markovic, J. Electroanal. Chem., 1982, 138, 443-447.

[22] R.R. Adzic, N.M. Markovic, V. B. Vesovic, J. Electroanal. Chem., 1984, 165, 105-120.

[23] R.R. Adzic, N.M. Markovic, V. B. Vesovic, J. Electroanal. Chem., 1984, 165, 121-133.

[24] N. M. Markovic, I. M. Tidswell, P. N. Ross, Langmuir, 1994, 10, 1-4.

[25] R. van Hardeveld, F. Hartog, Surface Science, 1969, 15, 189-230.

[26] P. Fischer, J. Heitbaum, J. Electroanal. Chem., 1980, 112, 231-238.

[27] L. Ardemani, G. Gibin, A.J.Dent, M.A.Isaacs, G. Kyriakou, A. F. Lee, C. M. A. Parlett, S.A.Parry, K. Wilson, Chem. Sci., 2015, 6, 4940-4945.

[28] C. Megías-Sayago, L.F. Bobadilla, S. Ivanova, A. Penkova, M.A. Centeno, J.A. Odriozola, Catal. Today , 2018, 301, 72–77.

[29] S. Strbac, R.R. Adzic, J. Electroanal. Chem., 1996, 403, 169-181.

[30] F. Hausen , J.A. Zimmet, R. Bennewitz, Surface Science, 2013, 607, 20–24.

[31] S. Kundu, Y. Wang, W. Xia, M. Muhler (2008) J. Phys. Chem. C 112, 16869–16878.

[32] A.Y Klyushin, R.Arrigo, Y. Youngmi, Z. Xie, M. Havecker, A.V. Bukhtiyarov, I.P. Prosvirin, V.I. Bukhtiyarov, A. Knop-Gericke, R. Schlogl, Topics Catal. 2016, 59, 469-477

[33] C.D. Wagner, D.A. Zatko, R.H. Raymond, Anal. Chem. **1980**, 52, 1445-1451

[34] G.P.Lopez, D.G. Castner, B.D. Ratner, Surf. Interface Anal., **1991**, 17, 267-272.

[35] J.L.Santos, M. Alda-Onggar, V. Fedorov, M. Peurla, K. Eränen, P. Mäki-Arvela, M. A. Centeno, D. Yu. Murzin, Appl. Catal. A, 2018, *561,* 137-149.

10.1002/cctc.201901742

FULL PAPER

Gold particle size strongly influences product selectivity and C balance during HMF oxidation reaction. Considering that oxygen reduction is thermodynamically favourable over Au (100) face, Au 100/111 exposure ratio is correlated with gold particle size and related with the observed FDCA selectivity, showing an indirect and clear dependence of the alcohol function oxidation with gold structure/size.

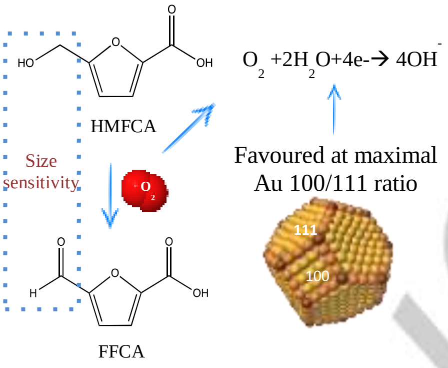

*C. Megías-Sayago, A. Lolli, D. Bonincontro, A. Penkova, S. Albonetti, F. Cavani, J. A. Odriozola and S. Ivanova**

Page No. – Page No.

Effect of gold particles size over Au/C catalyst selectivity in HMF oxidation reaction